Modelling of pellet ablation and homogenization for outboard side injection in the Large Helical Device

A. Matsuyama[1], F. Köchl[2], B. Pégourié[3], R. Sakamoto[1,4],
G. Motojima[1], J. S. Mishra[4], and H. Yamada[1,4]

[1]*National Institute for Fusion Science, Toki, 509-5292 Gifu, Japan*

[2]*Association EURATOM-ÖAW/ATI, Atominstitut, TU Wien, 1020 Vienna, Austria*

[3]*CEA, IRFM, F-13108 Saint-Paul-lez-Durance, France*

[4]*Graduate University for Advanced Studies, Toki, 509-5292 Gifu, Japan*

1. Introduction

Pellet injection is a promising fuelling scheme for achieving high-density operation relevant to fusion reactors. In tokamak experiments, the ∇B-induced drift displacements of the pellet deposited material play a major role for efficient fuelling with high-field side (HFS) injection. From experimental observation of drift down the magnetic field gradients in Large Helical Device (LHD) for outboard-side injection, it is suggested that similar mechanism exists also in stellarator/heliotron devices [1]. In this work, towards our goal to describe underlying physics of the pellet material deposition, we apply the modelling of pellet ablation and homogenization (the HPI2 code [2,3]) to outboard side injection for LHD.

2. Model description

LHD is a Heliotron device (where the poloidal and toroidal period numbers are L = 2 and M = 10) with a major radius R = 3.6-3.9 m, an average minor radius a = 0.6 m, and magnetic field up to 3 T. Hydrogen pellets are injected from outside midplane with the pipe-gun injector, where the injection speed is up to 1200 m/s. Experimentally, the penetration depth of the pellets has shown to be affected by fast ions produced by high-energy tangential NBI heating [4].

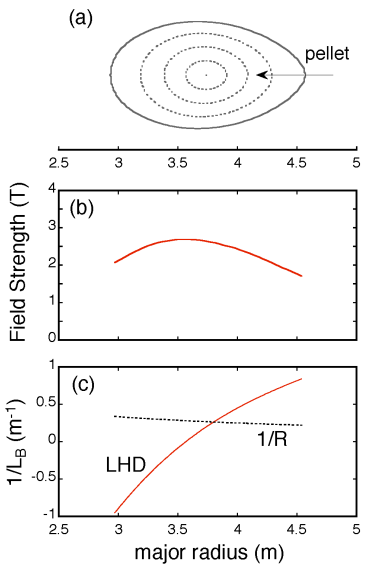

Figure 1. Radial field gradient for outboard side injection in LHD.

Figure 1 schematically shows radial structure of the magnetic field as functions of the major radius for outboard side injection. In early phase of the drift displacement, the deposited material drifts down the field gradient at the plasmoid center. In the LHD, the radial-gradient scale length L_B is characterized by minor radius; therefore, the drift acceleration term (which is proportional to

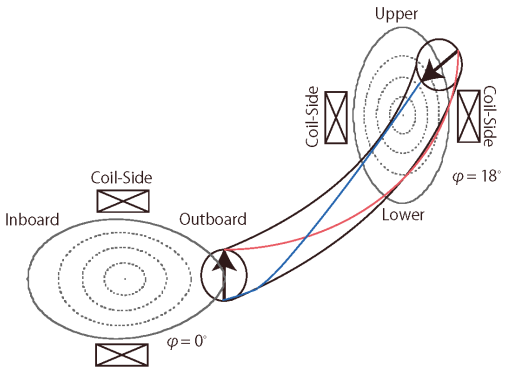

Figure 2. Schematic picture of the plasmoid internal parallel circuit. The connection with red and blue curves cancells the charge accumulation inside a plasmoid.

$1/L_B$) in the equation of motion of plasmoid is expected to be larger than for the LFS injection in tokamaks ($1/L_B \sim 1/R$). Nevertheless, it is suggested that the drift-damping mechanism due to internal parallel circuits [5] plays a key role in determining material deposition for timescale of pressure equilibration. (See Figure 2.) This effect is taken into account by the effective charge factor $A[L_0]$ prior to the drift acceleration term as

$$\frac{d\mathbf{V}_d}{dt} = A[L_0]\frac{2(p_0 - p_\infty)\nabla_\perp B}{n_0 m_i B}, \qquad (1)$$

where n_0 is the cloud density, m_i is ion mass, p_0 and p_∞ are the cloud and plasma pressure, respectively. The factor $A[L_0]$ is evaluated by taking average of ∇B current along the flux tube. Figure 3 compares the effective charge factor $A[L_0]$ for different radial location of plasmoid between LHD and a tokamak of the same aspect ratio. For axisymmetric tokamaks, $A[L_0] = (Rq/L_0)\sin(L_0/Rq)$ is analytically obtained if one neglects the poloidal field compared to the toroidal field $B_\theta << B_\varphi$. On the outer flux surfaces in the LHD, direction of the field gradient varies with rapid modulation of field strength due to helical coils. Therefore, even with relatively small toroidal expansion of plasmoid (whose characteristic scale length is qR/M) the internal parallel circuit effectively compensates the polarization charge and stops the drift acceleration towards the low-field side. For simulation, the expression of $A[L_0]$ specific to the LHD was introduced as well as magnetic-field parameters such as magnetic shear, which are relevant to the other stopping mechanisms: stopping by low-order rationals [6] and due to resistive currents flowing along flux tubes that connect the positively and negatively charged parts of plasmoid [3].

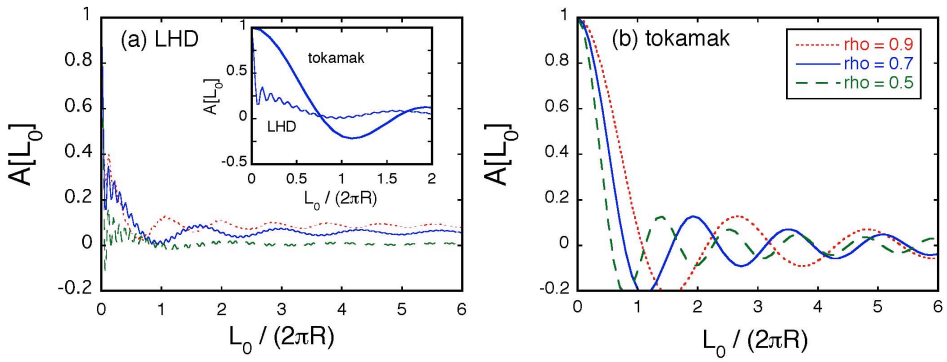

Figure 3. Comparison of effective charge factor $A[L_0]$ at different radial location of the plasmoid: (a) LHD and (b) a tokamak of the same aspect ratio.

3. Simulation for outboard side injection

In this work, we have developed two version of the code: (i) an ablation code taking into account realistic 3-D plasma shape of the LHD and (ii) the integrated simulation of ablation and homogenization with various machanisms of stopping the drift. Note that since it is still cumbersome to solve the whole fuelling process in full 3-D geometry, for the integrated simulation, helical field modulation of the LHD is approximately projected onto simple torus with circular cross section. In the both codes, effects of NBI heating on pellet penetration was considered for interpreting experimental penetrations.

In the LHD, the pellets are injected into NBI-heated plasmas, where fast ions enhance the ablation rate and reduce pellet penetration [4]. Our code can be applied to unbalance ablation during one-sided NBI heating, where the ablation rates for two sides of the pellet connecting to the field lines are solved independently. Figure 4 (a) illustrates the comparison between the code prediction and H_α emission for counter-clockwise NBI case, where $N_p = 6.2\times10^{20}$ atoms, V_p = 1.1 km/s, P_{inj} = 7.2 MW, $T_{e\infty}(\lambda_p)$ = 0.9 keV, and $n_{e\infty}(\lambda_p) = 5.4\times10^{19}$ m^{-3}. The code prediction is in good agreement with the penetration and the H_α emission profile. In Figure 4, the experimental penetration is around 60% shallower than the NGS prediction. Because of rather high energy of beam ions (~150-180 keV), the ablation rate is significantly enhanced [See Figure 4 (b)] on the side exposed to neutral beam in comparison to the opposite side.

The integrated simulation was performed for the first pellet injected into low density target plasmas, where $N_p = 2.2\times10^{21}$ atoms, V_p = 1.2 km/s, P_{inj} = 9.3 MW, $T_{e\infty}(\lambda_p)$ = 1.5 keV, and $n_{e\infty}(\lambda_p) = 1.3\times10^{19}$ m^{-3}. Figure 5 (a) shows the simulated mass-deposition and ablation profiles as well as the H_α emission. Because of outward displacements of individual plasmoid, 38 % loss of ablated mass was observed in simulation. Figure 5 (b) shows pre- and post-density profiles of simulation and experiment. Since only a density profile of 30 ms after injection is available for this pellet, we evaluated a density profile corresponding to the

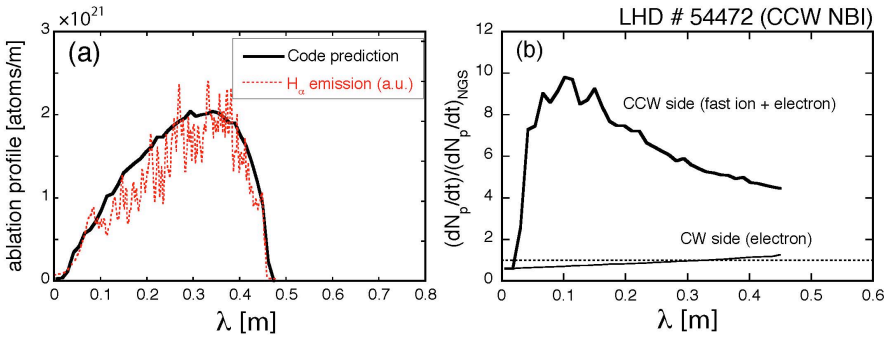

Figure 4. (a) Comparison between the simulated ablation profiles (—) and the H_α emission (- - - -, a.u.). (b) The ablation rates normalized by the NGS scaling for two sides of the pellet.

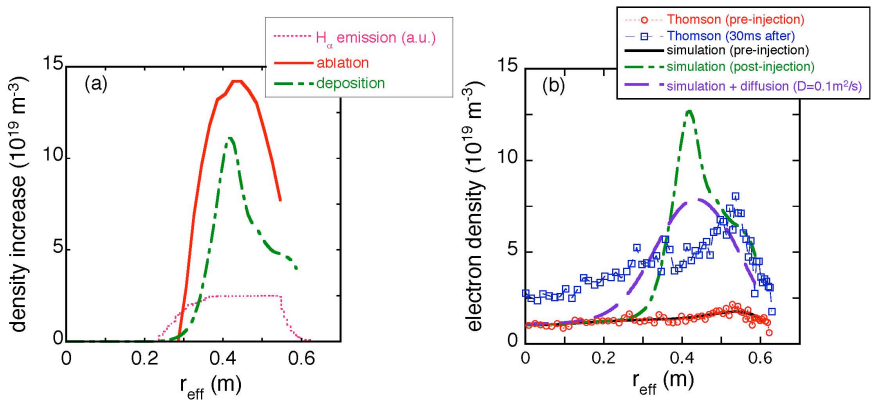

Figure 5. Comparison between the code prediction with experimental deposition for LHD no. 94527: (a) ablation and deposition profiles and (b) pre- and post-density profiles.

measurement from the diffusion equation, using the simulated particle source of Figure 5 (a), where $D = 0.1$ m^2/s is inferred from 0-D transport analysis. As a result, the fuelling efficiency of 51 % has been obtained for this case, which is in reasonable agreement to the observed values of 40-50 %. Since comparison of the main feature of deposition profiles, such as the shift between ablation and deposition profiles, is not straightforward for this timescale of diagnostics, the simulation will be compared with time-resolved Thomson scattering measurement in a subsequent work.

In summary, we have extended the modelling of pellet fuelling to the LHD for interpreting the ablation and homogenization process in stellarator/heliotron devices. In these devices, the effect of ∇B-induced drift displacements on the averaged depth of deposition profiles and the injection location that optimizes the fuelling efficiency have not yet been revealed. Detailed comparison between modelling and the LHD experiment contributes to the above purpose and also provides physics picture complementary to pellet ablation and homogenization in present-day tokamaks.

Acknowledgements

The authors acknowledge support by the LHD experiment group. This work was supported by NIFS10ULPP004, by Grants-in-Aid for Research Activity Start-Up 22860075 by Japan Society for Promotion of Science (JSPS), and in part by Grants-in-Aid Scientific Research (S) 20226018 by Ministry of Education, Culture, Sports, Science Society and Technology.

References

[1] R. Sakamoto, *et al*., Nucl Fusion **41**, 381 (2001).
[2] B. Pégourié, *et al*., Plasma Phys. Control. Fusion **47**, 17 (2005).
[3] B. Pégourié, *et al*., Nucl. Fusion **47**, 44 (2007).
[4] M. Hoshino, *et al*., Plasma Fusion Res. **1**, 033 (2006).
[5] V. A. Rozhansky, *et al*., Plasma Phys. Control. Fusion **46**, 575 (2004).
[6] N. Commaux, *et al*., Nucl. Fusion **50**, 025011 (2010).